Eur. Phys. J. C (2024) 84:1055
https://doi.org/10.1140/epjc/s10052-024-13435-9

THE EUROPEAN PHYSICAL JOURNAL C

Regular Article - Theoretical Physics

Pentaquark molecular states with hidden bottom and double strangeness

Jing Song[1,2,a], **Man-Yu Duan**[2,3,4,b], **Luis Roca**[5,c], **Eulogio Oset**[2,d]

[1] School of Physics, Beihang University, Beijing 102206, China
[2] Departamento de Física Teórica and IFIC, Centro Mixto Universidad de Valencia-CSIC Institutos de Investigación de Paterna, 46071 Valencia, Spain
[3] School of Physics, Zhengzhou University, Zhengzhou 450001, China
[4] School of Physics, Southeast University, Nanjing 210094, China
[5] Departamento de Física, Universidad de Murcia, 30100 Murcia, Spain

Received: 2 July 2024 / Accepted: 30 September 2024 / Published online: 14 October 2024

Abstract We investigate the meson-baryon interaction in coupled channels with the quantum numbers of the pentaquarks P_{bss} and P_{bsss}. The interaction is derived from an extension of the local hidden gauge approach to the heavy quark sector, which has demonstrated accurate results compared to experiments involving Ω_b, Ξ_b states, and pentaquarks P_c and P_{cs}. In our study, we identify several molecular states with small decay widths within the chosen set of coupled channels. The spin-parity (J^P) of these states is as follows: $J^P = \frac{1}{2}^-$ for pseudoscalar-baryon ($\frac{1}{2}^+$) coupled channels, $J^P = \frac{3}{2}^-$ for pseudoscalar-baryon ($\frac{3}{2}^+$) coupled channels, $J^P = \frac{1}{2}^-$ and $\frac{3}{2}^-$ for vector-baryon ($\frac{1}{2}^+$) coupled channels, and $J^P = \frac{1}{2}^-, \frac{3}{2}^-, \frac{5}{2}^-$ for vector-baryon ($\frac{3}{2}^+$) coupled channels. We search for the poles of these states and evaluate their couplings to the different channels.

1 Introduction

The collaborative efforts at contemporary hadron facilities are leading to the discovery of numerous new states with heavy quarks, some of which are evidently exotic and deviate from the standard quark model of $q\bar{q}$ for mesons and qqq for baryons. Specifically, there have been notable observations of baryons such as Λ_c [1–5], Σ_c [6], Ξ_c [7–13], Ω_c [14,15], Λ_b [16–20], Σ_b [21], Ξ_b [22–25], and Ω_b [26] (for a recent review of experimental findings, see Ref. [27]). Quark models have been extensively employed to study these states [28–46]. Furthermore, they have been investigated using lattice QCD techniques [38,47–52] and QCD sum rules [53–55]. Additional methods have also been applied in other studies [56–59]. The discovery of hidden charm pentaquarks P_c [60–62] and hidden charm pentaquarks with strangeness P_{cs} [63] has added significant excitement to the field. The search for new states is ongoing, and motivated by LHCb's plans to measure these new states, we focus here on the theoretical study of the P_{bss} and P_{bsss}.

The P_c and P_{cs} states have attracted significant attention in past research through various theoretical models. Quark model calculations of structures for these states have been carried out in [64–71].

Research on meson-baryon interactions is extensive, as reviewed in Refs. [72,73]. A successful approach involves exchanging vector mesons to predict various baryonic states with open charm or bottom quarks. For instance, the Ξ_{cc} states were examined in Ref. [74], and this was extended to Ξ_{bb} and Ω_{bbb} states in Ref. [75]. Studies on Ξ_c and Ξ_b states were conducted in Ref. [76], Ξ_{bc} states in Ref. [77], and Ω_b states in Ref. [78]. Some of these predicted states match recently discovered experimental states [27]. In particular, the predicted Ω_b states in Ref. [78] might correspond to observations reported in Ref. [26] as shown in Ref. [79]. Each study involves detailed analysis of interactions among multiple coupled channels.

Other studies also explore these states from a molecular perspective, using different methods and dynamics. For instance, in Ref. [80], researchers used one-pion exchange and $D^{(*)}$ exchange to study the dynamics of Ξ_{cc} states. In Ref. [81], heavy flavor, heavy quark spin, and heavy

[a] e-mail: Song-Jing@buaa.edu.cn (corresponding author)
[b] e-mail: duanmy@seu.edu.cn
[c] e-mail: luisroca@um.es
[d] e-mail: oset@ific.uv.es

antiquark–diquark symmetries are applied within an effective field theory framework to study pentaquarks and open bottom baryonic states. The one-boson exchange model is used to investigate Ω_c states in Ref. [82].

Moreover, extensive research has been conducted on molecular states arising from meson–baryon interactions in different sectors-light, charm, and bottom-using $SU(6)$lsf $\times$ $SU(2)$HQSS symmetry. This involves using $SU(6)$ flavor-spin symmetry in the light sector and $SU(2)$ in the heavy sector, while respecting heavy quark spin symmetry [83–85]. These studies extend the dynamics from the Weinberg-Tomozawa interaction and are noteworthy for their ability to correlate multiple coupled channels across different sectors. They make qualitative predictions for bound states and resonances with a wide range of quantum numbers. Recently, this approach has been used to address Ξ_b and Ξ_c states in Ref. [86].

Our goal is to investigate the states that can be formed as molecular states from the s-wave interaction of mesons with baryons in their ground state. Consequently, we expect to find only baryon states with negative parity. The attractive force between mesons and baryons often makes the formation of these states inevitable. Additionally, the proximity of the masses of some states to the threshold of certain meson–baryon channels necessitates the explicit consideration of these channels and their interactions in any comprehensive study of the baryon spectrum [87,88].

Many studies on molecular states in the charm sector have focused on the pentaquarks P_c, P_{cs}, and P_{css}. These states contain hidden charm, and have been reviewed in a number of papers [71,73,89–96], that also cover open heavy quark baryonic molecular states.

In the present paper we study baryon states with hidden bottom and two or three s quarks. The precursor of these states are the P_{css}, P_{csss}. The P_{css} states were studied from the molecular perspective, as meson baryon states in Refs. [94–96]. In Ref. [95] a pole was found for states of pseudoscalar-baryon($1/2^+$) nature (PB) and another one for states of vector-baryon($1/2^+$) nature (VB). In Ref. [96] such states were also found and, in addition, two more states of PB^* and VB^* nature were found with B^* corresponding to baryons of $3/2^+$. For the P_{csss}, of $c\bar{c}sss$ nature, no bound state was found. Similar results were found in Ref. [94], where, however, under certain circumstance the P_{csss} state could be also formed. It is important to mention that the dynamics of coupled channels was found essential to obtain the bound states, that were not generated in Refs. [97,98], where some important non diagonal channels were neglected.

In the present work we retake this line of research and look for possible states of $b\bar{b}ssq$ and $b\bar{b}sss$ nature. The only free parameter of the theory is constrained by the experimental results on the P_{cs} [63] and Ω_c [14,15] states that were studied along the same lines in Refs. [99,100], which should lead to reliable results in the predictions of $b\bar{b}ssq$ and $b\bar{b}sss$ involving arguments of heavy quark symmetry.

2 Formalism

We consider meson–baryon coupled channels: PB, VB, PB^*, and VB^*, where P represents the pseudoscalar meson, V denotes vector meson, B refers to ground state baryons with $J^P = \frac{1}{2}^+$, and B^* indicates ground state baryons with $J^P = \frac{3}{2}^+$. We do not mix these states as justified in Ref. [96] and discussed below.

(i) PB channels: $\eta_b \Xi^0$, $B_s^0 \Xi_b^{'}$, and $B^+\Omega_b^-$.
(ii) VB channels: $\Upsilon \Xi^0$, $B_s^{*0} \Xi_b^{'}$, and $B^{*+}\Omega_b^-$.
(iii) PB^* channels: $\eta_b \Xi^{*0}$, $B_s^0 \Xi_b^{*0}$, and $B^+\Omega_b^{*-}$.
(iv) VB^* channels: $\Upsilon \Xi^{*0}$, $B_s^{*0} \Xi_b^{*0}$, and $B^{*+}\Omega_b^{*-}$.
(v) PB^* : $\eta_b \Omega^-$, $B_s^0 \Omega_b^{*-}$
(vi) VB^* : $\Upsilon \Omega^-$, $B_s^{*0} \Omega_b^{*-}$

The first four sectors correspond to $b\bar{b}ssq$ states and the last two to $b\bar{b}sss$.

The interaction model we use is based on exchanging vector mesons, adapted from the local hidden gauge approach [101–105] to apply to the bottom sector [75–78,89,90,106]. To mix the interaction blocks, pion or other pseudoscalar exchanges are needed, but these contributions are much less significant than vector meson exchange when it comes to determining the masses of the states. While pion exchange can influence the widths of these states, in many cases where multiple channels are involved and the decay to lower mass states can happen via vector exchange, the effect of pion exchange is still relatively small (see the appendix of Ref. [107]). We focus on interactions in the S-wave, which helps define the J^P (spin-parity) characteristics of the states, and the relevant coupled channels are listed below in Table 1, together with their threshold masses.

As mentioned earlier, we use vector exchange based on an extended local hidden gauge approach between mesons and baryons, as shown in Fig. 1. For our set of states, there are two types of VMM' vertices: VPP (where V stands for vector and P stands for pseudoscalar) and VVV. These are described by the following Lagrangians [105]:

$$\mathcal{L}_{\rm VPP} = -ig\,\langle [P, \partial_\mu P]\, V^\mu \rangle, \tag{1}$$

$$\mathcal{L}_{\rm VVV} = ig\,\langle (V^\mu \partial_\nu V_\mu - \partial_\nu V^\mu V_\mu)\, V^\nu \rangle. \tag{2}$$

The coupling parameter g is determined by $g = \frac{m_V}{2f_\pi}$, where $m_V = 800$ MeV represents the vector meson mass and $f_\pi = 93$ MeV denotes the pion decay constant. In this context, P or V refer to the $q_i\bar{q}_j$ matrices expressed in terms of mesons. The symbol $\langle \cdots \rangle$ denotes the trace operation

Table 1 Threshold masses (in MeV) of different channels

PB, $J^P = \frac{1}{2}^-$	$\eta_b \Xi^0$	$B_s^0 \Xi_b^{'}$	$B^+ \Omega_b^-$
	10,713.6	11,301.9	11,324.5
VB, $J^P = \frac{1}{2}^-, \frac{3}{2}^-$	$\Upsilon \Xi^0$	$B_s^{*0} \Xi_b^{'}$	$B^{*+} \Omega_b^-$
	10,775.3	11,350.4	11,369.9
PB^*, $J^P = \frac{3}{2}^-$	$\eta_b \Xi^{*0}$	$B_s^0 \Xi_b^{*0}$	$B^+ \Omega_b^{*-}$
	10,930.5	11,319.2	11,381.3
VB^*, $J^P = \frac{1}{2}^-, \frac{3}{2}^-, \frac{5}{2}^-$	$\Upsilon \Xi^{*0}$	$B_s^{*0} \Xi_b^{*0}$	$B^{*+} \Omega_b^{*-}$
	10,992.2	11,367.7	11,426.7
PB^*, $J^P = \frac{3}{2}^-$	$\eta_b \Omega^-$	$B_s^0 \Omega_b^{*-}$	
	11,071.2	11,468.9	
VB^*, $J^P = \frac{1}{2}^-, \frac{3}{2}^-, \frac{5}{2}^-$	$\Upsilon \Omega^-$	$B_s^{*0} \Omega_b^{*-}$	
	11,132.9	11,517.4	

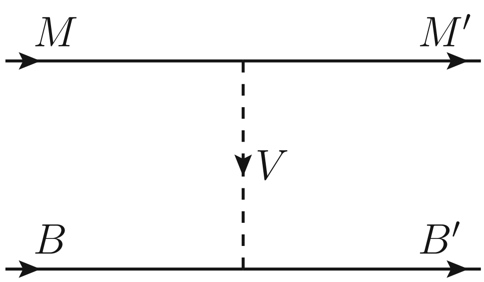

Fig. 1 The interaction between $MB \to M'B'$ happens through the exchange of vector mesons. Here $M(M')$ are the initial and final mesons, and $B(B')$ are the initial and final baryons. The vector meson involved in this exchange is represented by V

for these matrices. It is important to note that although $q_i \bar{q}_j$ matrices belong to the SU(4) or SU(5) groups, the vertices described in Eqs. (1) and (2) only involve the overlap of $q\bar{q}$ in the external mesons and the exchanged vectors. Therefore, the utilization of SU(4) or SU(5) symmetry is redundant, as discussed in Ref. [108].

The matrices P and V that we need are given by,

$$P = \begin{pmatrix} \frac{1}{\sqrt{2}}\pi^0 + \frac{1}{\sqrt{3}}\eta + \frac{1}{\sqrt{6}}\eta' & \pi^+ & K^+ & B^+ \\ \pi^- & -\frac{1}{\sqrt{2}}\pi^0 + \frac{1}{\sqrt{3}}\eta + \frac{1}{\sqrt{6}}\eta' & K^0 & B^0 \\ K^- & \bar{K}^0 & -\frac{1}{\sqrt{3}}\eta + \sqrt{\frac{2}{3}}\eta' & B_s^0 \\ B^- & \bar{B}^0 & \bar{B}_s^0 & \eta_b \end{pmatrix}, \tag{3}$$

$$V = \begin{pmatrix} \frac{1}{\sqrt{2}}\rho^0 + \frac{1}{\sqrt{2}}\omega & \rho^+ & K^{*+} & B^{*+} \\ \rho^- & -\frac{1}{\sqrt{2}}\rho^0 + \frac{1}{\sqrt{2}}\omega & K^{*0} & B^{*0} \\ K^{*-} & \bar{K}^{*0} & \phi & B_s^{*0} \\ B^{*-} & \bar{B}^{*0} & \bar{B}_s^{*0} & \Upsilon \end{pmatrix}. \tag{4}$$

Only the terms B, B_s and η_b of the P matrix enter the present calculation. The interaction obtained for the mechanism of Fig. 1 is always of the type

$$V_{ij} = g^2 (p_1^0 + p_3^0) C_{ij}, \tag{5}$$

where p_1^0, p_3^0 are the energies of the initial and final mesons, respectively. The coefficient C_{ij} are then evaluated and we find the following tables (Tables 2, 3, 4, 5) for these interactions.

After figuring out the V_{ij} potential, we use the Bethe-Salpeter equation expressed in matrix form to obtain the scattering matrix for the channels involved

$$T = [1 - VG]^{-1} V, \tag{6}$$

where G represents a diagonal matrix containing the loop functions for the intermediate states of meson and baryon. We adopt the cutoff approach to regularize the loops as outlined in Ref. [96], setting $q_{\max} = 600$ MeV. The l-th channel meson–baryon loop function, G_l, is given by

$$G_l(\sqrt{s}) = \int_{|q|<q_{\max}} \frac{d^3 q}{(2\pi)^3} \frac{2\, M_l\, (w_l(q) + E_l(q))}{2 w_l(q) E_l(q))} \times \frac{1}{s - (w_l(q) + E_l(q))^2 + i\epsilon}, \tag{7}$$

Table 2 Coefficients C_{ij} for the PB sector with $J^P = \frac{1}{2}^-$

States	$\eta_b \Xi^0$	$B_s^0 \Xi_b^{'}$	$B^+ \Omega_b^-$
$\eta_b \Xi^0$	0	$\frac{1}{\sqrt{6}} \frac{1}{M_{B_s^*}^2}$	$\frac{-1}{\sqrt{3}} \frac{1}{M_{B^*}^2}$
$B_s^0 \Xi_b^{'}$		$\frac{1}{M_\phi^2} - \frac{1}{M_\Upsilon^2}$	$\frac{\sqrt{2}}{M_{K^*}^2}$
$B^+ \Omega_b^-$			$-\frac{1}{M_\Upsilon^2}$

Table 3 Coefficients C_{ij} for the VB sector with $J^P = \frac{1}{2}^-, \frac{3}{2}^-$

States	$\Upsilon \Xi^0$	$B_s^{*0} \Xi_b^{'}$	$B^{*+} \Omega_c^0$
$\Upsilon \Xi^0$	0	$\frac{1}{\sqrt{6}} \frac{1}{M_{B_s^*}^2}$	$\frac{-1}{\sqrt{3}} \frac{1}{M_{B^*}^2}$
$B_s^{*0} \Xi_b^{'}$		$\frac{1}{M_\phi^2} - \frac{1}{M_\Upsilon^2}$	$\frac{\sqrt{2}}{M_{K^*}^2}$
$B^{*+} \Omega_c^0$			$-\frac{1}{M_\Upsilon^2}$

where M_l stands for the mass of the baryon, m_l for the meson and $w_l(q) = \sqrt{m_l^2 + \vec{q}^{\,2}}$, $E_l(q) = \sqrt{M_l^2 + \vec{q}^{\,2}}$. In the meson baryon rest frame, the total incident momentum P is $(\sqrt{s}, 0, 0, 0)$. [1]In the region of interest, the real part of G is negative.

Poles are encountered in the second Riemann sheet, necessitating a change from the loop function in the first sheet, G^I, to that in the second one, G^{II}, as follows:

$$G_j^{II} = G_j^I + i \frac{2M_j q}{4\pi \sqrt{s}}, \tag{8}$$

for Re$\sqrt{s} > m_j + M_j$, and q given by

$$q = \frac{\lambda^{1/2}(s, m_j^2, M_j^2)}{2\sqrt{s}}, \quad (\text{Im } q > 0). \tag{9}$$

We further assess the couplings defined by the residue at the pole position, $\sqrt{s_P}$, where the amplitudes behave as:

$$T_{ij} = \frac{g_i g_j}{\sqrt{s} - \sqrt{s_P}}. \tag{10}$$

If the pole is not too far from the real axis, $\sqrt{s_P}$ can be associated to the mass, M, and width, Γ, of the generated state by $\sqrt{s_P} \simeq M + i\Gamma/2$. For one g_i, we select a sign, while the remaining couplings have their relative signs well defined. Additionally, we present $g_i G_i^{II}$, yielding the wave function at the origin in coordinate space [110].

Moreover, we can assess the compositeness, denoted as X_i, of a generated resonance in a given channel, i. This value indicates the weight of a molecular component in the state i in the wave function, as described in Refs. [110–112].

$$\chi_i = - g_i^2 \frac{\partial G_i}{\partial \sqrt{s_P}}\bigg|_{\sqrt{s_P}}. \tag{11}$$

where the derivative is done at the pole of the state in the complex plane.

We call this magnitude"weight" and not probability as done in many works, because this magnitude is in general complex. Only if we have a bound state which does not decay, this magnitude corresponds to a probability. The precise meaning of this magnitude is explained in Ref. [113] (sections 5 and 6 of that reference) and it corresponds to the integral of the square of the wave function with a certain phase prescription, which only gets contribution from the confined region of the particles and not from the asymptotic wave function of the decay modes. However, in our case, since the decay widths are so small, it is fair to identify χ_i with the probability of finding the particles.

[1] For some channels far below the energy under consideration, it is common to consider only Im G, which has repercussion on the widths, and neglect Re G [109]. We follow a slightly different prescription taking Re G=0 when Re G becomes bigger than 0 and use the exact Im G.

Table 4 Coefficients C_{ij} for the PB sector with $J^P = \frac{3}{2}^-$

States	$\eta_b \Xi^{*0}$	$B_s^0 \Xi_b^{*0}$	$B^+ \Omega_b^{*-}$
$\eta_b \Xi^{*0}$	0	$\frac{\sqrt{2}}{\sqrt{3}} \frac{1}{M_{B_s^*}^2}$	$\frac{1}{\sqrt{3}} \frac{1}{M_{B^*}^2}$
$B_s^0 \Xi_b^{*0}$		$\frac{1}{M_\phi^2} - \frac{1}{M_\Upsilon^2}$	$\frac{\sqrt{2}}{M_{K^*}^2}$
$B^+ \Omega_b^{*-}$			$-\frac{1}{M_\Upsilon^2}$

Table 5 Coefficients C_{ij} for the VB sector with $J^P = \frac{1}{2}^-, \frac{3}{2}^-, \frac{5}{2}^-$

States	$\Upsilon \Xi^{*0}$	$B_s^{*0} \Xi_b^{*0}$	$B^{*+} \Omega_b^{*-}$
$\Upsilon \Xi^{*0}$	0	$\frac{\sqrt{2}}{\sqrt{3}} \frac{1}{M_{B_s^*}^2}$	$\frac{1}{\sqrt{3}} \frac{1}{M_{B^*}^2}$
$B_s^{*0} \Xi_b^{*0}$		$\frac{1}{M_\phi^2} - \frac{1}{M_\Upsilon^2}$	$\frac{\sqrt{2}}{M_{K^*}^2}$
$B^{*+} \Omega_b^{*-}$			$-\frac{1}{M_\Upsilon^2}$

Table 6 Coefficients C_{ij} for the PB^* sector with $J^P = \frac{3}{2}^+, \frac{3}{2}^-$

States	$\eta_b \Omega^-$	$B_s^0 \Omega_b^{*-}$
$\eta_b \Omega^-$	0	$\frac{1}{M_{B_s^*}^2}$
$B_s^0 \Omega_b^{*-}$		$\frac{2}{M_\phi^2} - \frac{1}{M_\Upsilon^2}$

Table 7 Coefficients C_{ij} for the VB^* sector with $J^P = \frac{3}{2}^+, \frac{3}{2}^-, \frac{5}{2}^-$

States	$\Upsilon \Omega^-$	$B_s^{*0} \Omega_b^{*-}$
$\Upsilon \Omega^-$	0	$\frac{1}{M_{B_s^*}^2}$
$B_s^{*0} \Omega_b^{*-}$		$\frac{2}{M_\phi^2} - \frac{1}{M_\Upsilon^2}$

Table 8 PB states (pole position in units of MeV). The first row in poles, g_i and χ_i correspond to $q_{\max} = 600$ MeV and the second one to $q_{\max} = 800$ MeV. χ_i stands for compositeness. The last column is the sum of the different compositeness

Poles		$\eta_b \Xi^0$	$B_s^0 \Xi_b^{'}$	$B^+ \Omega_b^-$	
(11,259.7 − i0.16)	g_i	(0.12 + i0.00)	(− 2.62 − i0.01)	(4.03 + i0.01)	
(11,166.0 − i0.36)		(0.19 − i0.00)	(− 4.30 − i0.00)	(5.98 + i0.01)	
	χ_i	(− 0.00 + i0.00)	(0.42 − i0.00)	(0.57 + i0.00)	(0.99 − i0.00)
		(− 0.00 + i0.00)	(0.38 − i0.00)	(0.60 − i0.00)	(0.98 − i0.00)

Table 9 Same as Table 8 for VB states

Poles		$\Upsilon \Xi^0$	$B_s^{*0} \Xi_b^{'}$	$B^{*+} \Omega_b^-$	
(11,306.2 − i0.16)	g_i	(0.12 + i0.00)	(− 2.67 − i0.01)	(4.02 + i0.01)	
(11,212.3 − i0.35)		(0.19 − i0.00)	(− 4.35 − i0.01)	(5.99 + i0.01)	
	χ_i	(− 0.00 + i0.00)	(0.41 − i0.00)	(0.58 + i0.00)	(0.99 − i0.00)
		(− 0.00 + i0.00)	(0.38 − i0.00)	(0.60 − i0.00)	(0.98 − i0.00)

Table 10 Same as Table 8 for PB^* states

Poles		$\eta_b \Xi^{*0}$	$B_s^0 \Xi_b^{*0}$	$B^+ \Omega_b^{*-}$	
(11,297.8 − i0.01)	g_i	(0.03 + i0.00)	(− 1.99 − i0.00)	(4.35 − i0.00)	
(11,206.6 − i0.00)		(0.02 + i0.00)	(− 3.94 − i0.00)	(6.23 − i0.00)	
	χ_i	(− 0.00 + i0.00)	(0.52 + i0.00)	(0.47 − i0.00)	(0.99 + i0.00)
		(− 0.00 + i0.00)	(0.42 + i0.00)	(0.56 − i0.00)	(0.98 + i0.00)

When searching for pole positions, employing $G_l^I(\sqrt{s})$ for $\mathrm{Re}(\sqrt{s}) < m_l + M_l$ and $G_l^{II}(\sqrt{s})$ for $\mathrm{Re}(\sqrt{s}) > m_l + M_l$ brings us closer to the pole positions and half-widths akin to those of the corresponding Breit-Wigner forms along the real axis. This method also aids in identifying potential pure bound states situated below the lowest threshold, where the prescription of Eq. (8) with the $\mathrm{Re}\sqrt{s} > M_l + m_l$ renders us to the first Riemann sheet (Tables 6, 7).

3 Results

In Tables 8, 9, 10, 11 we show the results obtained using $q_{\max} = 600$ MeV and $q_{\max} = 800$ MeV.

As we can see in the Table 8, for the PB channel, we get a bound state with extremely small width. The state couples mostly both to $B_s^0 \Xi_b^{'}$ and $B^+ \Omega_b^-$, and for $q_{\max} = 600$ MeV,

Table 11 Same as Table 8 for VB^* states

Poles		$\Upsilon \Xi^{*0}$	$B_s^{*0} \Xi_b^{*0}$	$B^{*+} \Omega_b^{*-}$	
(11,344.6 − i0.01)	g_i	(0.03 + i0.00)	(− 2.06 − i0.00)	(4.36 − i0.00)	
(11,253.0 − i0.00)		(0.02 + i0.00)	(− 3.99 − i0.00)	(6.24 − i0.00)	
	χ_i	(− 0.00 + i0.00)	(0.51 + i0.00)	(0.48 − i0.00)	(0.99 + i0.00)
		(− 0.00 + i0.00)	(0.41 + i0.00)	(0.57 − i0.00)	(0.98 + i0.00)

Table 12 Summary of states obtained. Results with $q_{\max} = 600$ MeV are shown. The binding is defined with respect to the lowest mass bound coupled channels (first channel in the column of main channels, see thresholds in Table 1)

State [MeV]	Binding [MeV]	J^P	Main channels
11,259.7 − i0.16	42.2	$1/2^-$	$B_s^0 \Xi_b^{'}$, $B^+ \Omega_b^-$
11,306.2 − i0.16	44.2	$1/2^-, 3/2^-$	$B_s^{*0} \Xi_b^{'}$, $B^{*+} \Omega_b^-$
11,297.8 − i0.01	21.4	$3/2^-$	$B_s^0 \Xi_b^{*0}$, $B^+ \Omega_b^{*-}$
11,344.6 − i0.01	23.1	$1/2^-, 3/2^-, 5/2^-$	$B_s^{*0} \Xi_b^{*0}$, $B^{*+} \Omega_b^{*-}$

it is bound by about 40 MeV with respect to the $B_s^0 \Xi_b'$ threshold and couples very weakly to the $\eta_b \Xi^0$, the only channel open for decay, hence the small width obtained. The wave functions at the origin follow the same trend as the couplings. Table 9 shows results for the VB states, very similar to those of the PB case. The main couplings are to $B_s^{*0} \Xi_b'$ and $B^{*+} \Omega_b^-$, and the $\Upsilon \Xi^0$ has a small coupling, leading to a very small width. The results are also similar in the PB^* and VB^* channels in Tables 10 and 11.

We show also the results for $q_{\max} = 800$ MeV to have a feeling for uncertainties, but the value of $q_{\max} = 600$ MeV is closer to the one used to get the Ω_c in Ref. [99] and P_{cs} states in Ref. [100]. According to [114–116], implementing heavy quark symmetry demands the use of the same cut off in the charm and bottom sectors. The interesting thing is that in all four cases we get a bound state with very small width (Table 12).

We give now some words about the probabilities found for each channels χ_i. The values of χ_i are complex, because we have small widths from the decay channels. As mentioned before, in this case the proper interpretation of the meaning of χ_i can be seen in Ref. [113]. However, given the very small imaginary parts, the interpretation of the real part as a measure of the probability to find the given component in the wave function is appropriate. We find the total probability close to 1 indicating the molecular component of the states, which is natural from their construction. In the triple strangeness sector we do not find bound states. We do not even get cusps around thresholds, which would indicate the failure, but the proximity, to have a bound state.

4 Conclusions

We have addressed the issue of possible pentaquark states of type $b\bar{b}ssq$ and $b\bar{b}sss$ of molecular nature, stemming from the interaction of mesons with baryons in their ground state. We have considered four types of such states coming from the interaction of PB, VB, PB^*, VB^*, where P stands for pseudoscalar mesons, V for vector mesons and B, B^* for baryons of $1/2^+$ and $3/2^+$ respectively. We have made implicit use of heavy quark symmetry using cutoff regularization of the loops with the same cutoff in the bottom sector as in the charm sector [114–116]. We have then relied upon the analysis of the Ω_c and P_{cs} states along the same lines as in the present work to get reasonably values of this cutoff. We obtain bound states of $b\bar{b}ssq$ type, with an extremely small width, for each of these four sectors, which are bound by about 50 MeV. We have also addressed the $b\bar{b}sss$ sector, but in this case we do not find any bound state. We are looking forward to future experimental search of these states in LHCb or other facilities. The work presented here not only shows the existence of these states, but also the open channels where they decay, which should serve as guidance for future experiments.

Acknowledgements This work is partly supported by the National Natural Science Foundation of China under Grants and no. 12405089 and no. 12247108 and the China Postdoctoral Science Foundation under Grant no. 2022M720360 and no. 2022M720359. This work is partly supported by the Spanish Ministerio de Economia y Competitividad (MINECO) and European FEDER funds under Contracts no. FIS2017-84038-C2-1-P B, PID2020-112777GB-I00, and by Generalitat Valenciana under contract PROME-TEO/2020/023. This project has received funding from the European Union Horizon 2020 research and innovation programme under the program H2020-INFRAIA-2018-1, Grant agreement no. 824093 of the STRONG-2020 project.

Data Availability Statement This manuscript has no associated data. [Authors' comment: All data generated during this study are contained in this published article.]

Code Availability Statement This manuscript has no associated code/software. [Authors' comment: Code/Sotware sharing not applicable to this article as no code/sofware was generated or analysed during the current study.]

References

1. K.W. Edwards et al. (CLEO), Phys. Rev. Lett. **74**, 3331 (1995)
2. H. Albrecht et al. (ARGUS), Phys. Lett. B **317**, 227 (1993)
3. M. Artuso et al. (CLEO), Phys. Rev. Lett. **86**, 4479 (2001)
4. R. Aaij et al. (LHCb), JHEP **05**, 030 (2017)
5. B. Aubert et al. (BaBar), Phys. Rev. Lett. **98**, 012001 (2007)
6. R. Mizuk et al. (Belle), Phys. Rev. Lett. **94**, 122002 (2005)
7. S.E. Csorna et al. (CLEO), Phys. Rev. Lett. **86**, 4243 (2001)
8. J.P. Alexander et al. (CLEO), Phys. Rev. Lett. **83**, 3390 (1999)
9. B. Aubert et al. (BaBar), Phys. Rev. D **77**, 031101 (2008)
10. R. Aaij et al. (LHCb), Phys. Rev. Lett. **124**, 222001 (2020)
11. R. Chistov et al. (Belle), Phys. Rev. Lett. **97**, 162001 (2006)
12. T.J. Moon et al. (Belle), Phys. Rev. D **103**, L111101 (2021)
13. B. Aubert et al. (BaBar), Phys. Rev. D **77**, 012002 (2008)
14. R. Aaij et al. (LHCb), Phys. Rev. Lett. **118**, 182001 (2017)
15. R. Aaij et al. (LHCb), Phys. Rev. Lett. **131**, 131902 (2023)
16. R. Aaij et al. (LHCb), Phys. Rev. Lett. **109**, 172003 (2012)
17. T.A. Aaltonen et al. (CDF), Phys. Rev. D **88**, 071101 (2013)
18. A.M. Sirunyan et al. (CMS), Phys. Lett. B **803**, 135345 (2020)
19. R. Aaij et al. (LHCb), JHEP **06**, 136 (2020)
20. R. Aaij et al. (LHCb), Phys. Rev. Lett. **123**, 152001 (2019)
21. R. Aaij et al. (LHCb), Phys. Rev. Lett. **122**, 012001 (2019)
22. A.M. Sirunyan et al. (CMS), Phys. Rev. Lett. **126**, 252003 (2021)

23. R. Aaij et al. (LHCb), Phys. Rev. Lett. **121**, 072002 (2018)
24. R. Aaij et al. (LHCb), Phys. Rev. D **103**, 012004 (2021)
25. R. Aaij et al. (LHCb), Phys. Rev. Lett. **128**, 162001 (2022)
26. R. Aaij et al. (LHCb), Phys. Rev. Lett. **124**, 082002 (2020)
27. H.-X. Chen, W. Chen, X. Liu, Y.-R. Liu, S.-L. Zhu, Rep. Prog. Phys. **86**, 026201 (2023)
28. S.S. Gershtein, V.V. Kiselev, A.K. Likhoded, A.I. Onishchenko, Mod. Phys. Lett. A **14**, 135 (1999)
29. S.S. Gershtein, V.V. Kiselev, A.K. Likhoded, A.I. Onishchenko, Phys. Rev. D **62**, 054021 (2000)
30. D. Ebert, R.N. Faustov, V.O. Galkin, A.P. Martynenko, Phys. Rev. D **66**, 014008 (2002)
31. V.V. Kiselev, A.K. Likhoded, O.N. Pakhomova, V.A. Saleev, Phys. Rev. D **66**, 034030 (2002)
32. W. Roberts, M. Pervin, Int. J. Mod. Phys. A **23**, 2817 (2008)
33. A. Valcarce, H. Garcilazo, J. Vijande, Eur. Phys. J. A **37**, 217 (2008)
34. C. Albertus, E. Hernandez, J. Nieves, Phys. Lett. B **683**, 21 (2010)
35. C. Albertus, E. Hernandez, J. Nieves, Phys. Rev. D **85**, 094035 (2012)
36. Y.-L. Ma, M. Harada, Phys. Lett. B **748**, 463 (2015)
37. Z. Shah, K. Thakkar, A.K. Rai, Eur. Phys. J. C **76**, 530 (2016)
38. H. Garcilazo, A. Valcarce, J. Vijande, Phys. Rev. D **94**, 074003 (2016)
39. Q.-F. Lü, K.-L. Wang, L.-Y. Xiao, X.-H. Zhong, Phys. Rev. D **96**, 114006 (2017)
40. L.-Y. Xiao, Q.-F. Lü, S.-L. Zhu, Phys. Rev. D **97**, 074005 (2018)
41. J.-J. Niu, L. Guo, H.-H. Ma, X.-G. Wu, X.-C. Zheng, Phys. Rev. D **98**, 094021 (2018)
42. N. Salehi, N. Mohajery, Eur. Phys. J. Plus **133**, 416 (2018)
43. Q. Li, C.-H. Chang, S.-X. Qin, G.-L. Wang, Chin. Phys. C **44**, 013102 (2020)
44. L.X. Gutiérrez-Guerrero, A. Bashir, M.A. Bedolla, E. Santopinto, Phys. Rev. D **100**, 114032 (2019)
45. Z. Shah, A. Kakadiya, K. Gandhi, A.K. Rai, Universe **7**, 337 (2021)
46. Z. Ghalenovi, C.-P. Shen, M. Moazzen Sorkhi, Phys. Lett. B **834**, 137405 (2022)
47. R. Lewis, N. Mathur, R.M. Woloshyn, Phys. Rev. D **64**, 094509 (2001)
48. H.-W. Lin, Chin. J. Phys. **49**, 827 (2011)
49. Z.S. Brown, W. Detmold, S. Meinel, K. Orginos, Phys. Rev. D **90**, 094507 (2014)
50. P. Pérez-Rubio, S. Collins, G.S. Bali, Phys. Rev. D **92**, 034504 (2015)
51. H. Bahtiyar, K.U. Can, G. Erkol, M. Oka, T.T. Takahashi, Phys. Rev. D **98**, 114505 (2018)
52. R.A. Briceno, H.-W. Lin, D.R. Bolton, Phys. Rev. D **86**, 094504 (2012)
53. Z.-G. Wang, Eur. Phys. J. A **45**, 267 (2010)
54. X.-H. Hu, Y.-L. Shen, W. Wang, Z.-X. Zhao, Chin. Phys. C **42**, 123102 (2018)
55. Z.-G. Wang, Eur. Phys. J. C **78**, 826 (2018)
56. M.H. Weng, X.H. Guo, A.W. Thomas, Phys. Rev. D **83**, 056006 (2011)
57. M. Karliner, J.L. Rosner, Phys. Rev. Lett. **115**, 122001 (2015)
58. J. Soto, J. Tarrús Castellà, Phys. Rev. D **102**, 014013 (2020) [Erratum: Phys. Rev. D 104, 059901 (2021)]
59. J. Soto, J. Tarrús Castellà, Phys. Rev. D **104**, 074027 (2021)
60. R. Aaij et al. (LHCb), Phys. Rev. Lett. **115**, 072001 (2015)
61. R. Aaij et al. (LHCb), Phys. Rev. Lett. **122**, 222001 (2019)
62. R. Aaij et al. (LHCb), Phys. Rev. Lett. **128**, 062001 (2022)
63. R. Aaij et al. (LHCb), Sci. Bull. **66**, 1278 (2021)
64. L. Maiani, A.D. Polosa, V. Riquer, Phys. Lett. B **749**, 289 (2015)
65. S. Takeuchi, M. Takizawa, Phys. Lett. B **764**, 254 (2017)
66. Y. Yamaguchi, A. Giachino, A. Hosaka, E. Santopinto, S. Takeuchi, M. Takizawa, Phys. Rev. D **96**, 114031 (2017)
67. Y. Yamaguchi, E. Santopinto, Phys. Rev. D **96**, 014018 (2017)
68. Y. Yamaguchi, H. García-Tecocoatzi, A. Giachino, A. Hosaka, E. Santopinto, S. Takeuchi, M. Takizawa, Phys. Rev. D **101**, 091502 (2020)
69. M. Karliner, J.L. Rosner, Sci. Bull. **66**, 1257 (2021)
70. E. Santopinto, A. Giachino, Phys. Rev. D **96**, 014014 (2017)
71. Y.-R. Liu, H.-X. Chen, W. Chen, X. Liu, S.-L. Zhu, Prog. Part. Nucl. Phys. **107**, 237 (2019)
72. J.A. Oller, E. Oset, A. Ramos, Prog. Part. Nucl. Phys. **45**, 157 (2000)
73. F.-K. Guo, C. Hanhart, U.-G. Meißner, Q. Wang, Q. Zhao, B.-S. Zou, Rev. Mod. Phys. **90**, 015004 (2018) [Erratum: Rev. Mod. Phys. 94, 029901 (2022)]
74. J.M. Dias, V.R. Debastiani, J.J. Xie, E. Oset, Phys. Rev. D **98**, 094017 (2018)
75. J.M. Dias, Q.-X. Yu, W.-H. Liang, Z.-F. Sun, J.-J. Xie, E. Oset, Chin. Phys. C **44**, 064101 (2020)
76. Q.X. Yu, R. Pavao, V.R. Debastiani, E. Oset, Eur. Phys. J. C **79**, 167 (2019)
77. Q.-X. Yu, J.M. Dias, W.-H. Liang, E. Oset, Eur. Phys. J. C **79**, 1025 (2019)
78. W.-H. Liang, J.M. Dias, V.R. Debastiani, E. Oset, Nucl. Phys. B **930**, 524 (2018)
79. W.-H. Liang, E. Oset, Phys. Rev. D **101**, 054033 (2020)
80. Y. Shimizu, M. Harada, Phys. Rev. D **96**, 094012 (2017)
81. F.-K. Guo, C. Hidalgo-Duque, J. Nieves, M.P. Valderrama, Phys. Rev. D **88**, 054014 (2013)
82. R. Chen, A. Hosaka, X. Liu, Phys. Rev. D **97**, 036016 (2018)
83. O. Romanets, L. Tolos, C. Garcia-Recio, J. Nieves, L.L. Salcedo, R.G.E. Timmermans, Phys. Rev. D **85**, 114032 (2012)
84. C. Garcia-Recio, J. Nieves, O. Romanets, L.L. Salcedo, L. Tolos, Phys. Rev. D **87**, 074034 (2013)
85. C. Garcia-Recio, J. Nieves, O. Romanets, L.L. Salcedo, L. Tolos, Phys. Rev. D **87**, 034032 (2013)
86. J. Nieves, R. Pavao, L. Tolos, Eur. Phys. J. C **80**, 22 (2020)
87. X.-K. Dong, F.-K. Guo, B.S. Zou, Few Body Syst. **62**, 61 (2021)
88. V. Baru, X.-K. Dong, M.-L. Du, A. Filin, F.-K. Guo, C. Hanhart, A. Nefediev, J. Nieves, Q. Wang, Phys. Lett. B **833**, 137290 (2022)
89. X.-K. Dong, F.-K. Guo, B.-S. Zou, Commun. Theor. Phys. **73**, 125201 (2021)
90. X.-K. Dong, F.-K. Guo, B.-S. Zou, Progr. Phys. **41**, 65 (2021)
91. H.-X. Chen, W. Chen, X. Liu, S.-L. Zhu, Phys. Rep. **639**, 1 (2016)
92. Y. Dong, A. Faessler, V.E. Lyubovitskij, Prog. Part. Nucl. Phys. **94**, 282 (2017)
93. A. Ramos, A. Feijoo, Q. Llorens, G. Montaña, Few Body Syst. **61**, 34 (2020)
94. F.-L. Wang, R. Chen, X. Liu, Phys. Rev. D **103**, 034014 (2021)
95. J.A. Marsé-Valera, V.K. Magas, A. Ramos, Phys. Rev. Lett. **130**, 091903 (2023)
96. L. Roca, J. Song, E. Oset, Phys. Rev. D **109**, 094005 (2024)
97. J.-J. Wu, R. Molina, E. Oset, B.S. Zou, Phys. Rev. C **84**, 015202 (2011)
98. C.W. Xiao, J. Nieves, E. Oset, Phys. Rev. D **88**, 056012 (2013)
99. V.R. Debastiani, J.M. Dias, W.H. Liang, E. Oset, Phys. Rev. D **97**, 094035 (2018)
100. A. Feijoo, W.-F. Wang, C.-W. Xiao, J.-J. Wu, E. Oset, J. Nieves, B.-S. Zou, Phys. Lett. B **839**, 137760 (2023)
101. M. Bando, T. Kugo, S. Uehara, K. Yamawaki, T. Yanagida, Phys. Rev. Lett. **54**, 1215 (1985)
102. M. Bando, T. Kugo, K. Yamawaki, Phys. Rep. **164**, 217 (1988)
103. M. Harada, K. Yamawaki, Phys. Rep. **381**, 1 (2003)
104. U.G. Meissner, Phys. Rep. **161**, 213 (1988)
105. H. Nagahiro, L. Roca, A. Hosaka, E. Oset, Phys. Rev. D **79**, 014015 (2009)

106. S.-Y. Kong, J.-T. Zhu, D. Song, J. He, Phys. Rev. D **104**, 094012 (2021)
107. J.M. Dias, G. Toledo, L. Roca, E. Oset, Phys. Rev. D **103**, 116019 (2021)
108. S. Sakai, L. Roca, E. Oset, Phys. Rev. D **96**, 054023 (2017)
109. L. Dai, G. Toledo, E. Oset, Eur. Phys. J. C **80**, 510 (2020)
110. D. Gamermann, J. Nieves, E. Oset, E. Ruiz Arriola, Phys. Rev. D **81**, 014029 (2010)
111. L.R. Dai, J. Song, E. Oset, Phys. Lett. B **846**, 138200 (2023)
112. J. Song, L.R. Dai, E. Oset, Phys. Rev. D **108**, 114017 (2023)
113. F. Aceti, L.R. Dai, L.S. Geng, E. Oset, Y. Zhang, Eur. Phys. J. A **50**, 57 (2014)
114. J.-X. Lu, Y. Zhou, H.-X. Chen, J.-J. Xie, L.-S. Geng, Phys. Rev. D **92**, 014036 (2015)
115. M. Altenbuchinger, L.S. Geng, W. Weise, Phys. Rev. D **89**, 014026 (2014)
116. A. Ozpineci, C.W. Xiao, E. Oset, Phys. Rev. D **88**, 034018 (2013)